

Fluence Dependence of Charge Collection of irradiated Pixel Sensors

T. Rohe ^{a,1} D. Bortoletto ^b V. Chiochia ^c L. M. Cremaldi ^d
 S. Cucciarelli ^e A. Dorokhov ^{c,a} C. Hoermann ^{a,c} D. Kim ^f
 M. Konecki ^e D. Kotlinski ^a K. Prokofiev ^{c,a} C. Regenfus ^c
 D. A. Sanders ^d S. Son ^b T. Speer ^c M. Swartz ^f

^a*Paul Scherrer Institut, 5232 Villigen PSI, Switzerland*

^b*Purdue University - Task G, West Lafayette, IN 47907, USA*

^c*Physik Institut der Universität Zürich-Irchel, 8057 Zürich, Switzerland*

^d*Department of Physics and Astronomy, University of Mississippi, University, MS 38677, USA*

^e*Institut für Physik der Universität Basel, 4056 Basel, Switzerland*

^f*Johns Hopkins University, Baltimore, MD 21218, USA.*

Presented at the 5th Int. Conf. on Radiation Effects on Semiconductor Materials
 Detectors and Devices, October 10-13, 2004 in Florence, Italy

Abstract

The barrel region of the CMS pixel detector will be equipped with “n-in-n” type silicon sensors. They are processed on DOFZ material, use the moderated p-spray technique and feature a bias grid. The latter leads to a small fraction of the pixel area to be less sensitive to particles. In order to quantify this inefficiency prototype pixel sensors irradiated to particle fluences between 4.7×10^{13} and 2.6×10^{15} n_{eq}/cm² have been bump bonded to un-irradiated readout chips and tested using high energy pions at the H2 beam line of the CERN SPS. The readout chip allows a non zero suppressed analogue readout and is therefore well suited to measure the charge collection properties of the sensors.

In this paper we discuss the fluence dependence of the collected signal and the particle detection efficiency. Further the position dependence of the efficiency is investigated.

Key words: LHC, CMS, tracking, pixel, silicon, radiation hardness.

¹ Corresponding author; e-mail: Tilman.Rohe@cern.ch

1 Introduction

The CMS experiment, currently under construction at the Large Hadron Collider (LHC) at CERN (Geneva, Switzerland), will contain a hybrid pixel detector for tracking and vertexing [1]. In its final configuration it will consist of three barrel layers and two end disks at each side.

To improve the spatial resolution analogue interpolation between neighboring channels will be performed. The strong Lorentz deflection in the radial direction caused by CMS' 4 T magnetic field is used to distribute the signal over two and more pixels. For this reason the pixel size of $100 \times 150 \mu\text{m}^2$ was chosen. In the disks, where the charge carrier drift is minimally affected by the magnetic field, the modules are tilted by about 20° with respect to the plane orthogonal to the beam line to induce charge sharing between pixels.

Because of the harsh radiation environment at the LHC, the technical realization of the pixel detector is very challenging. The innermost barrel layer will be exposed to a fluence of about $3 \times 10^{14} \text{ n}_{\text{eq}}/\text{cm}^2$ per year at the full LHC-luminosity, the second and third layer to about $1.2 \times 10^{14} \text{ n}_{\text{eq}}/\text{cm}^2$ and $0.6 \times 10^{14} \text{ n}_{\text{eq}}/\text{cm}^2$, respectively. All components of the pixel detector are specified to remain operational up to a particle fluence of at least $6 \times 10^{14} \text{ n}_{\text{eq}}/\text{cm}^2$. This implies that parts of the detector will have to be replaced during the lifetime of the experiment. In case of a possible luminosity upgrade of the LHC the particle fluences will be much increased and it has to be investigated up to which particle fluence the detectors can be operated. The life time of the sensor is limited by insufficient charge collection caused by trapping and incomplete depletion. As both effects can be reduced by increasing the sensor bias, the choice of the sensor concept must allow the operation at high bias voltages without causing electrical breakdown. For the CMS pixel detector a maximum value of 500-600 V is foreseen.

In addition to the radiation-induced bulk effects the charge collection properties of the sensor are also influenced by the pixel design (e.g. the implant geometry). Therefore, the design has to be optimized to minimize potential regions with reduced signal collection. The aim of this study is to investigate the fluence and position dependence of the charge collection properties in the CMS prototype sensors.

2 The CMS Pixel Barrel Sensors

For the sensors of the pixel detector the “*n-in-n*” concept has been chosen. Electron collection has the advantage that after irradiation induced space

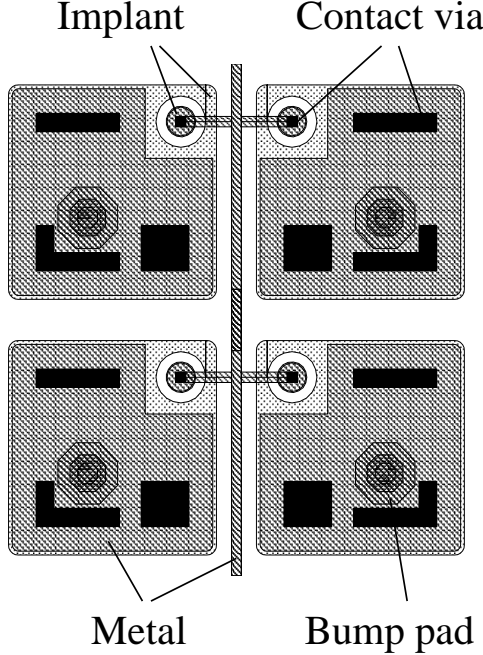


Fig. 1. Mask layout of the pixel sensors under study.

charge sign inversion, the highest electric field is located close to the collecting electrodes. In addition double-sided processing of these devices allows the implementation of guard rings only on the *p*-side of the sensor, keeping all sensor edges at ground potential. The design of the guard rings has been optimized in the past [2]. The breakdown voltage exceeds safely the required value of 600 V.

Due to the superior performance after irradiation and the possibility to implement a bias grid the moderated *p*-spray technique was chosen for the pixel barrel [3]. The pixel layout is shown in Fig. 1 and is characterized by small gaps of 20 μm between the n^+ -implants and by a biasing structure implementing small punch through “bias dots” [4]. They allow on wafer current-voltage (IV) measurements and keep accidentally unconnected pixel cells close to ground potential. Following the recommendation of the ROSE collaboration [5], oxygen enriched silicon was used to improve the post irradiation behavior. The thickness of the sensors was $285 \pm 15 \mu\text{m}$.

The pixel size of the sensors investigated in this study was $125 \times 125 \mu\text{m}^2$ in order to match the readout chip. Although these dimensions differ from the ones foreseen in CMS we are confident that the basic charge collection properties presented in this paper are not affected by the cell size. Other properties, e.g. the spatial resolution, have to be measured with the final configuration.

3 Testing Procedure

In a pixelated device the parameters important for the performance of a single channel, like pixel capacitance and leakage current, are independent of the array dimensions. Therefore the use of miniature sensors does not restrict the validity of the results. The results presented in this paper were obtained with sensors containing 22×32 pixels.

After the deposition of the under bump metalization and the indium bumps the sensors were diced. Some of them were irradiated at the CERN PS with 24 GeV protons² with fluences between 0.47 and $26 \times 10^{14} \text{ n}_{\text{eq}}/\text{cm}^2$ (see tab. 1). The irradiation was performed without cooling and bias.

In order to avoid reverse annealing the sensors were stored at -20°C after irradiation and warmed up only for transport and bump bonding. Some of the samples were annealed for three days at 30° close to the minimum of the full depletion voltage [6]. To sort out defective sensors all of them were characterized with IV-measurements before and after irradiation.

Several miniature sensors were bump bonded to readout chips of the type PSI30/AC30³ described in detail in [7]. This chip was chosen instead of the final CMS-pixel readout chip because it allows a sequential readout of all pixel cells without zero suppression. The sampling time at the shaper was defined by an external hold signal provided by a pin-diode with a delay of about 60 ns. The peaking times of the preamplifier and the shaper were adjusted to about 40 ns by tuning the feedback resistors of the charge sensitive amplifiers. This setting prevents saturation of the preamplifier and shaper up to signals corresponding to about 1.5 minimal ionizing particles (m.i.p.) but leads to a higher noise. As the readout chip is not sufficiently radiation hard, irradiated sensors were bump bonded to un-irradiated readout chips. Therefore a special bump bonding procedure without heat application was used.

The bump bonded samples were tested at the CERN-SPS H2 beam line using 150 GeV pions in 2003 and 2004. The pixel device under test was situated in-between a four layer silicon strip telescope [8] with an intrinsic spatial resolution of about $1 \mu\text{m}$. The sensors were cooled to a temperature of -10°C by water cooled Peltier elements. The whole set-up was placed in a 3 T magnet with the \vec{B} field parallel to the beam (2003) or perpendicular (2004). The pixel detector was set either normal to the beam (90°), tilted by a small angle ($75 - 110^\circ$), or tilted to an angle of 15° between the beam and the sensor

² hardness factor 0.62 [5]

³ PSI30 DMILL pixel readout chip was designed in 1997 at Paul Scherrer Institut, Villigen, Switzerland, and translated in 1998 to the Honeywell RICMOS IV process at 1. Physikalischs Institut of the RWTH Aachen, Germany.

surface.

The data recorded at an impact angle of 15° are also used for modeling charge drift and trapping in heavily irradiated sensors [9,10], and to measure the Lorentz angle [11] and the electric field within the sensors [12].

4 Signal Height

The analogue information obtained from the readout chip was used to study the signal height as a function of the sensor bias and the irradiation fluence. To avoid saturation of the signal data was taken at an angle of 15° between the beam and the sensor surface. As the pitch is more than two times smaller than the sensor thickness the collected charge per pixel is about 10000 electrons (most probable value) for an unirradiated sensor. The tilt of the sensor was such that the long clusters (“streets”) run parallel to the pixel columns. The telescope information was used to select streets which run along the center of a column. By this charge sharing between neighboring pixel columns was avoided. Further this excludes the two regions of reduced charge collection, the bias dot and the metal line running along every second pixel column (see fig. 1) from the analysis. The charge of all pixels along the street was summed applying a threshold of 2000 electrons. The charge distribution was fitted with a Gaussian convoluted with a Landau. For each fluence and bias voltage the most probable value was divided by the one obtained with an unirradiated sensor at 150 V.

Figure 2 shows this ratio as a function of the detector bias for several fluences. The data were not corrected for possible differences in wafer thickness or non-uniformities in the preamplifier gains which are estimated to be at the few percent level. The increase of the ratio faster than with the square root of the bias, typical for the “n-in-n” detectors after the irradiation induced space-charge sign-inversion (so called “type inversion”), is nicely visible. At the bias usually referred to as “full depletion” voltage the signal saturates.

The sensor irradiated to a fluence of $\Phi = 2.6 \times 10^{15} \text{ n}_{\text{eq}}/\text{cm}^2$ could only be operated up a maximum voltage of 600 V at -10° C . At higher voltages the readout chip became very noisy. Therefore small data samples were recorded at 750 V and 900 V at -25° C to suppress the leakage current. The signal at this voltages were slightly higher than at 600 V.

Figure 2 was used to determine the best bias voltage for sensor operation. The spatial resolution very much depend on the charge sharing between neighbor-

⁴ Using a pixel threshold of 2 k electrons

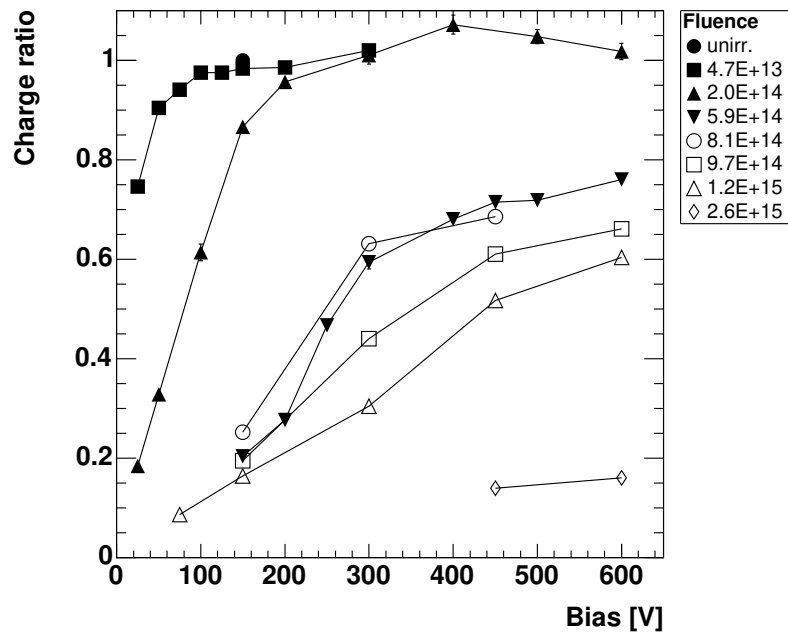


Fig. 2. Most probable signal as a function of the sensor bias. The signal of the un-irradiated sensor at 150 V is used as reference.

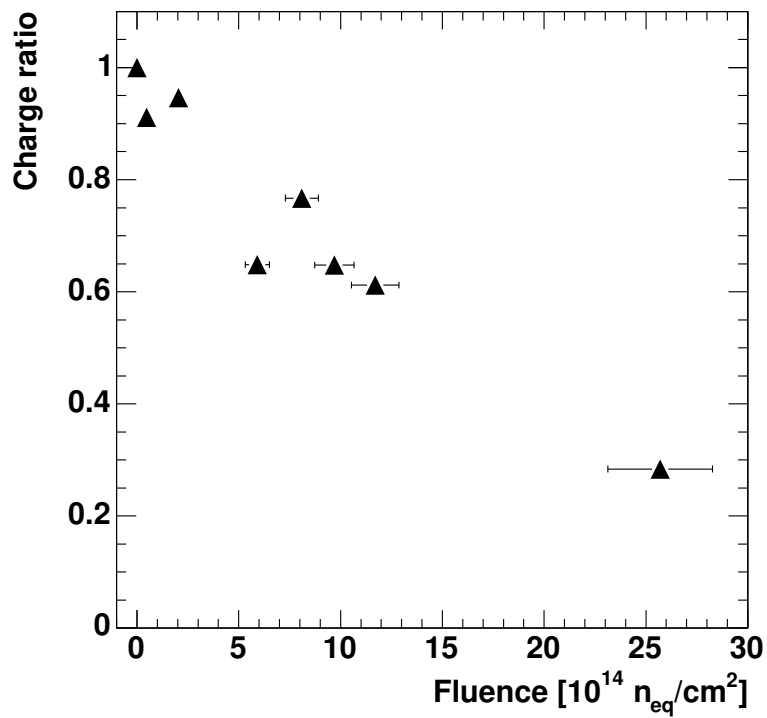


Fig. 3. Most probable signal as function of the irradiation fluence.

Φ [10^{14} n _{eq} /cm ²]	Bias [V]	Charge ratio		Efficiency	
		[mip]	[ke ⁻]	0 T	3 T
0	150	1	22.4	> 0.999	> 0.999
0.47	100	0.91	20.3	> 0.999	> 0.999
2.0	200	0.95	21.3	0.995	0.994
5.9	400	0.65	14.6	0.989	0.990
8.0	450	0.77	17.2	0.988	
9.7	600	0.65	14.6	0.990	
11.7	600	0.61	13.7	0.956	0.980
25.7	600	0.28	6.3	0.924 ⁴	

Table 1

Operation voltage and measured charge ratios for the sensors irradiated to different fluences. From this number the expected absolute charge is calculated. The detection efficiency is obtained using a pixel threshold of 3 k electrons.

ing channels caused by the Lorentz deflection in the magnetic field. As the Lorentz angle decreases with a higher bias [11] the lowest bias voltage with a “full” signal collection was selected. The chosen voltages are listed in Tab. 1. For those voltages large data samples were recorded with the beam normal with respect to the sensor surface. The telescope prediction was used to select events in the pixel center in order to avoid charge sharing and to exclude areas with reduced charge collection. The charge distribution of the pixels predicted by the telescope was also fitted with a Gaussian convoluted with a Landau and the most probable value obtained from the fit was divided by the one obtained with an unirradiated sensor at 150 V. The values of these charge ratios are also listed in Tab. 1.

Figure 3 shows the charge ratio as a function of the fluence. In the fluence range relevant for CMS ($0 - 12 \times 10^{14}$ n_{eq}/cm²) the signal sensor will be above 12 k electrons which is sufficient for a reliable operation. The signal of the highly irradiated sensor (2.6×10^{15} n_{eq}/cm²) is very close to the limits of readout electronics which are presently available.

5 Detection Efficiency

In [3] it was shown that the bias dot and the and, after irradiation, the region of the metal line running along every second pixel column have a reduced charge collection. Similar results have also been reported from other pixel detectors using a punch through dot [13]. Those regions, which were excluded

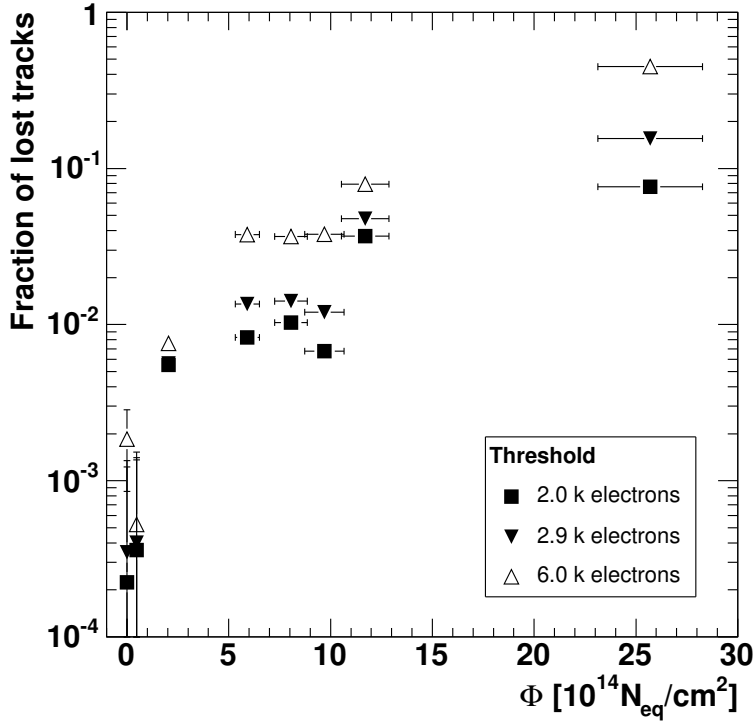


Fig. 4. Fraction of lost hits as function of the hadron fluence.

in the analysis shown in the previous section, degrade the performance of the detector. There is a chance that a particle that crosses the sensor in this region causes a signal too small to exceed the threshold of a sparcified readout.

To determine the effect of those regions on the sensor performance data taken with a normal incidence angle were used. The beam telescope is used to precisely predict the impact position on the sensor. If the pixel predicted by the telescope or a direct neighbor is above a certain threshold the track was counted as detected. Due to dead time of the DAQ system the measured efficiency has a systematic error which was estimated to about 0.1 %.

Figure 4 shows the dependence of the detection inefficiency of the sensors listed in tab. 1 on the radiation fluence for pixel thresholds of 2, 3 and 6 k electrons without magnetic field. Typically a threshold of 2-3 k electrons is applied. For fluences below $10^{15} \text{ n}_{\text{eq}}/\text{cm}^2$ and a threshold below 3 k electrons the fraction of lost tracks is well below 2 %, even with a threshold of 6 k electrons it does not exceed 5 %.

The signal of the sensor irradiated to $2.6 \times 10^{15} \text{ n}_{\text{eq}}/\text{cm}^2$ has the most probable value of only about 6.2 k electrons. For a reliable operation of this sensor a threshold lower than this value is necessary. With 2 k electrons an efficiency of better than 90 % is reached. For higher thresholds the efficiency decreased

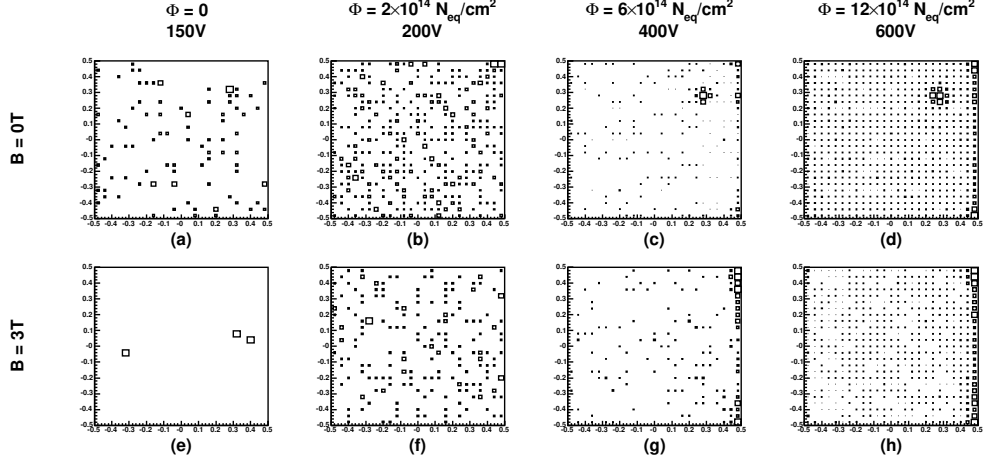


Fig. 5. Position of the tracks not detected by the pixel sensor for data recorded with (lower row) and without magnetic field (upper row). Each plot represents the area of one pixel shown in fig. 1. The bias dot is located in the top right corner, the aluminum line is placed along the right edge. The pixel threshold is set to 3 k electrons.

rapidly. The noise of this detector was very high ($\approx 1000 e^-$). However it was to a large extend caused by the fact that the readout chips was not designed to accept such a high leakage current. Future measurements with sensors irradiated to such high fluences will be carried out with modified readout chips featuring an appropriate leakage current compensation.

The position of the lost hits within the pixel cell is shown in fig. 5 for different fluences and data with and without magnetic field. For the un-irradiated sensor and the one irradiated to $2 \times 10^{14} n_{eq}/cm^2$ the hits below the threshold of 3 k electrons, are uniformly distributed over the pixel area (see fig. 5a and b). This means that the charge collected in the less efficient regions is still safely above this threshold. If the threshold is increased to about 6 k electrons the undetected hits start to be concentrated in the region of the bias dot.

For the devices with an irradiation fluence above a few $10^{14} n_{eq}/cm^2$ the collected charge is significantly reduced by trapping. Additional losses due to incomplete charge collection lead to an increased inefficiency. Hence the undetected hits are concentrated at the bias dot and along the aluminum line (see fig. 5c and d). However, the total number of lost hits is small.

If a 3 T magnetic field parallel to the horizontal axis of the histograms in fig. 5 is applied, the charge carriers are deflected by the Lorentz force which is parallel to the vertical axis. This leads to a distribution of the deposited charge along the vertical axis and reduces the influence of the small bias dot. Therefore the concentration of undetected hits around the bias dot is not present in fig. 5e–h. If a threshold of 6 k electrons is applied a slightly smeared “image” of the bias dot becomes visible in the highly irradiated sensors. As the

Lorentz drift of the signal charge is parallel to the aluminum line, the number of undetected tracks in this region is not effected by the magnetic field as visible in fig. 5c, d, g and h. The total detection efficiency of the sensors is not changed by the application of the magnetic field within the errors (see tab. 1). It is still in a tolerable range below 5%.

6 Conclusions

Silicon pixel sensors of *n*-in-*n*type featuring moderated *p*-spray isolation have been irradiated up to proton fluences of $2.6 \times 10^{15} \text{ n}_{\text{eq}}/\text{cm}^2$. The charge collection studies were performed with bump bonded samples using a high energy pion beam. The total charge collected after $1.2 \times 10^{15} \text{ n}_{\text{eq}}/\text{cm}^2$ and a bias of 600 V was about 60% compared to an unirradiated sample. After $2.6 \times 10^{15} \text{ n}_{\text{eq}}/\text{cm}^2$ about 28% of the original signal could be collected. This result is very encouraging with respect to possible upgrade scenarios for LHC.

The detection efficiency of the sensors is above 95% up to an irradiation fluence of $1.2 \times 10^{15} \text{ n}_{\text{eq}}/\text{cm}^2$ using a pixel threshold of 3 k electrons and a bias voltage of 600 V. The bias dot and the aluminum line connecting pixels originate the major source of inefficiency. The influence of the dot is reduced if a magnetic field parallel to the sensor surface is applied.

The tested sensors fulfill all requirements of the CMS experiment and will be used in the barrel section of the pixel detector.

Acknowledgments

The authors would like to thank Silvan Streuli from ETH Zürich and Fredy Glaus from PSI for their enormous effort in bump bonding, Kurt Bösiger from the workshop of the University of Zürich for the mechanical construction, Maurice Glaser, Michael Moll, and Federico Ravotti from CERN for carrying out the irradiation, Waclaw Karpinski from RWTH Aachen for providing the last existing wafer of front-end chips, György Bencze and Pascal Petiot from CERN for the H2-beam line support.

References

- [1] The CMS Collaboration. CMS Tracker. Technical Design Report LHCC 98-6, CERN, Geneva, Switzerland, 1998.

- [2] R. Kaufmann. *Development of radiation hard pixel sensors for the CMS experiment*. PhD thesis, Universität Zürich, Switzerland, 2001.
- [3] T. Rohe et al. Position dependence of charge collection in prototype sensors for the CMS pixel detector. *IEEE Trans Nucl Sci*, 51 (3):1150–1157, 2004.
- [4] T. Rohe for the ATLAS Pixel Collaboration. Design and test of pixel sensors for the ATLAS pixel detector. *Nucl. Instrum. Methods*, A 460:55–66, 2001.
- [5] G. Lindström et al. Radiation hard silicon detectors – developments by the RD48 (ROSE) collaboration. *Nucl. Instrum. Methods*, A 466:308–326, 2001.
- [6] M. Moll, G. Lindström, et al. LHC-scenario, spread sheet. private communication, 2003.
- [7] D. Meer. Bau und Messen eines Multichip Pixelmodules als Prototyp für den CMS-Tracker. Diplomarbeit, Eidgenössische Technische Hochschule, Zürich, Switzerland, March 2000.
- [8] C. Amsler et al. A high resolution beam telescope. *Nucl. Instrum. Methods*, A 480:501–507, 2002.
- [9] M. Swartz et al. Type inversion in irradiated silicon: a half truth. e-print [physics/0409049], 2004.
- [10] V. Chiochia et al. Simulation of heavily irradiated silicon pixel sensors and comparison with test beam measurements. Presented at the IEEE NSS, Oct. 16-22, 2004, Rome, Italy. Submitted for publication in IEEE-TNS. e-print [physics/0411143].
- [11] A. Dorokhov et al. Test of silicon sensors for the cms pixel detector. *Nucl. Instrum. Methods*, A 530:71–76, 2004.
- [12] A. Dorokhov et al. Pixel sensors under heavy irradiation. Presented at Vertex 2004, Sept. 13-18, 2004, Menaggio-Como, Italy. Submitted for publication in NIM A.
- [13] T. Lari for the ATLAS Pixel Collaboration. Test beam results of ATLAS pixel sensors. In *Proceedings of the International Workshop on Semiconductor Pixel Detectors for Particles and X-Rays (PIXEL2002)*, 2002. <http://www.slac.stanford.edu/econf/C020909/>.

B = 0 T

